A GRID CONNECTED PHOTOVOLTAIC GENERATION SYSTEM WITH HARMONIC AND REACTIVE POWER COMPENSATION

M. C. Cavalcanti, G. M. S. Azevedo, K. C. de Oliveira, B. A. Amaral, F. A. S. Neves, Z. D. Lins
Departamento de Engenharia Elétrica e Sistemas de Potência – Universidade Federal de Pernambuco
Rua Acadêmico Hélio Ramos s/n – Cidade Universitária, CEP 50.740-530, Recife – PE - Brasil
e-mail: marcelo.cavalcanti@ufpe.br, gustavo.azevedo@ufpe.br, kleber.oliveira@ufpe.br, fneves@ufpe.br, zdl@ufpe.br

Abstract – **This paper presents a system that provides photovoltaic generation, current harmonic compensation and reactive power compensation. A single-stage configuration is simulated, resulting in increased efficiency. A synchronous reference frame based controller is compared to an instantaneous reactive power based controller. The synchronous reference frame method is chosen to control the inverter due to the better performance when the grid voltage waveform is distorted. The maximum power point controller allows tracking the maximum power point very rapidly. Computer simulations demonstrate the good performance of the system for different pulse-width-modulation techniques.**

Keywords - **Converter control, Power Quality, Renewable energy systems, Solar Cell Systems, Three phase systems, Vector control.**

I. INTRODUCTION

Photovoltaic (PV) energy has great potential to supply energy with minimum impact on the environment, since it is clean and pollution free [1]. One way of using photovoltaic energy is in a distributed energy system as a peaking power source [2]. The distributed generation systems using PV energy are especially interesting when batteries are not used as energy storage elements. In this case, there is a considerable reduction in the system costs and increase of permanency time in operation. The permanency time has great influence in the life-cycle-cost of the PV energy generation systems [3]. To increase the PV system utilization the power conversion can be designed to also provide current harmonic compensation and reactive power compensation.

The elements that compose the power conversion of the solar panels to the load and the grid have great influence in the operation of the PV energy generation systems [4]. Conventionally, grid connected photovoltaic energy conversion systems are composed of a dc-dc converter and an inverter [5]. The efficiency of the system is low because the dc-dc converter and the inverter are in series. The voltage source inverter is the usually proposed alternative for connection of the PV energy generation systems to the grid [6, 7]. Operation feature of the grid connected PV generation system is strongly dependent on the algorithm employed to control the inverter. It has been shown that synchronous reference frame (SRF) controller [8] and instantaneous reactive power (IRP) theory based compensators [9] achieve significant performance for implementation.

This paper presents the design of a photovoltaic generation system for connection in a three-phase grid using only one inverter. The proposed design increases efficiency and reduces size. The system provides photovoltaic generation, current harmonic compensation and reactive power compensation. A synchronous reference frame method [8] is compared to an instantaneous reactive power based controller [9] and the synchronous reference frame method is chosen to control the three-phase inverter. The maximum power point tracking (MPPT) controller allows reaching the maximum power point very rapidly [1]. The system has been simulated and different pulse-width-modulation (PWM) techniques have been compared to suggest a control with high efficiency.

II. SYNCHRONOUS REFERENCE FRAME CONTROLLER

Figure 1 shows the block diagram of the proposed system. The converter is responsible to convert the PV energy to the grid as well as to compensate current harmonics and reactive power.

The complete model of the system (Fig. 1) in the *123* referential is shown in (1) [8]:

$$\frac{d}{dt}\begin{bmatrix} i_1 \\ i_2 \\ i_3 \\ V \end{bmatrix} = \begin{bmatrix} -\frac{R}{L} & 0 & 0 & -\frac{d_1}{L} \\ 0 & -\frac{R}{L} & 0 & -\frac{d_2}{L} \\ 0 & 0 & -\frac{R}{L} & -\frac{d_3}{L} \\ \frac{d_1}{C} & \frac{d_2}{C} & \frac{d_3}{C} & 0 \end{bmatrix} \cdot \begin{bmatrix} i_1 \\ i_2 \\ i_3 \\ V \end{bmatrix} + \frac{1}{L}\begin{bmatrix} v_1 \\ v_2 \\ v_3 \\ 0 \end{bmatrix} \tag{1}$$

Where:

i_1, i_2, i_3	- Three-phase inverter currents.
V	- PV array output voltage.
R, L	- Resistance and inductance of the transformer.
d_1, d_2, d_3	- Three-phase switching state functions.
C	- Capacitance of the dc link.
v_1, v_2, v_3	- Three-phase grid voltages.

In (1), the steady state fundamental components are sinusoidal. To reduce control complexity, the *d-q* frame in (2) rotating at the supply frequency can be used. With this frame, the positive-sequence components at fundamental frequency become constant [8]:

$$\begin{bmatrix} i_d \\ i_q \\ i_0 \end{bmatrix} = \sqrt{\frac{2}{3}}\begin{bmatrix} \cos\omega t & \cos(\omega t - 2\pi/3) & \cos(\omega t + 2\pi/3) \\ -sin\omega t & -sin(\omega t - 2\pi/3) & -sin(\omega t + 2\pi/3) \\ 1/\sqrt{2} & 1/\sqrt{2} & 1/\sqrt{2} \end{bmatrix} \cdot \begin{bmatrix} i_1 \\ i_2 \\ i_3 \end{bmatrix} \tag{2}$$

Where:

i_d, i_q	- D-axis and q-axis inverter currents.
i_0	- Zero-sequence inverter current.
ω	- Grid angular frequency.

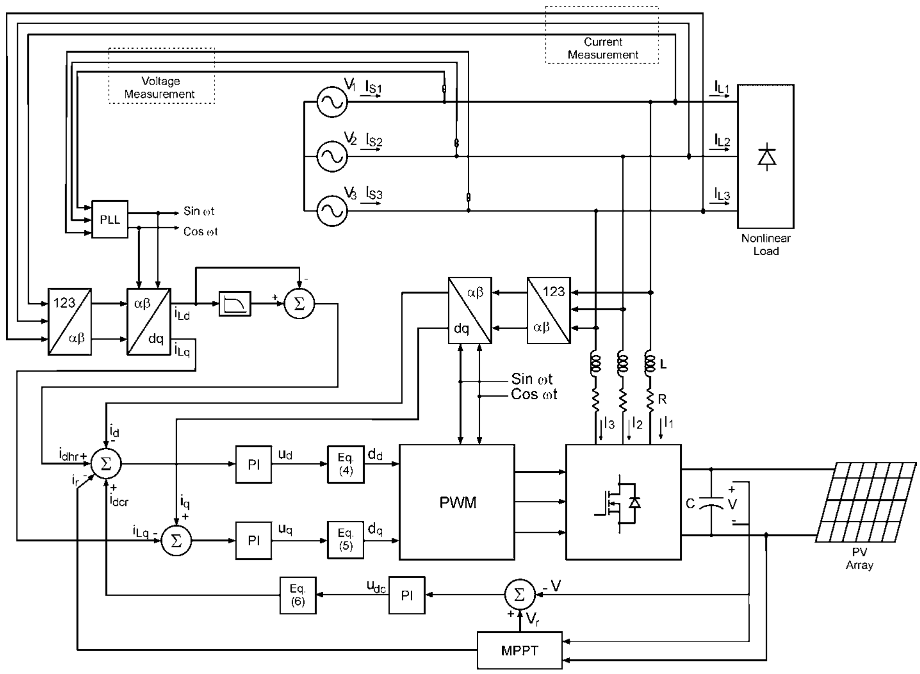

Fig. 1. Block diagram of the synchronous reference frame based controller for the proposed system.

Taking into account the absence of the zero-sequence components in the currents in a three-wire system, the model in the *dq* frame is as in (3) [8]:

$$\frac{d}{dt}\begin{bmatrix} i_d \\ i_q \\ V \end{bmatrix} = \begin{bmatrix} -R/L & \omega & -d_d/L \\ -\omega & -R/L & -d_q/L \\ d_d/C & d_q/C & 0 \end{bmatrix} \cdot \begin{bmatrix} i_d \\ i_q \\ V \end{bmatrix} + \frac{1}{L}\begin{bmatrix} v_d \\ v_q \\ 0 \end{bmatrix} \tag{3}$$

Where:

d_d, d_q - D-axis and q-axis switching state functions.
v_d, v_q - D-axis and q-axis grid voltages.

The current and voltage controls are realized by using PI compensators. The phase-locked-loop (PLL) circuit detects the amplitude and the position of the grid voltage vector. When the system is operating as photovoltaic energy generator, the MPPT controller is used to calculate the reference voltage. When the system is operating only as current harmonic and reactive power compensator, the reference voltage is constant [1].

In the SRF, the fundamental positive-sequence components of the load appear as dc quantities [8]. Since the grid currents must have a sinusoidal waveform and be in phase with the grid voltage in the proposed design, the grid current has only d-axis component. Therefore, the q-axis reference current for the inverter is the q-axis load current [2]. The d-axis reference current is composed of three parts: d-axis reference current of the load (i_{dhr}), reference current of the dc link (i_{dcr}) and reference current of the PV array (i_{pvr}). The d-axis current of the load is passed through a low pass filter that removes the high frequency components in the *d-q* reference frame. A first order low pass filter with a cut frequency of 20Hz is used. Subtracting the d-axis load current of the filtered d-axis load current, the result is the negative of the d-axis harmonics. This value is used as the reference d-axis load current since the positive current flows into the inverter. The dc component in the *d-q* reference frame corresponds to the fundamental component of the real power flowing to the load. The inverter dc link voltage controller calculates the current to maintain the dc link voltage by passing the dc link voltage error through a PI compensator. This current is added to the current to maintain the dc link voltage. The current obtained by the MPPT controller corresponds to the real power available from the photovoltaic array and it is subtracted from the other current components.

The control of the system is based on the development realized in [8] and (4), (5) and (6) in Fig. 1 are:

$$d_d = \frac{v_d + L\cdot\omega\cdot i_q - u_d}{V} \tag{4}$$

$$d_q = \frac{v_q - L\cdot\omega\cdot i_d - u_q}{V} \tag{5}$$

$$i_{dcr} = \sqrt{\frac{2}{3}}\frac{V\cdot u_{dc}}{V_{grid}} \tag{6}$$

Where:

u_d, u_q - Outputs of the current PI compensators.
i_{dcr} - Reference current of the dc link.
u_{dc} - Output of the voltage PI compensator.
V_{grid} - Amplitude of the grid voltage.

Using *d-q* reference frame, the coupled dynamics of the current tracking problem have been transformed into decoupled dynamics.

III. INSTANTANEOUS REACTIVE POWER CONTROLLER

To realize the harmonic and reactive power compensation, it can be used the concept of instantaneous active and reactive power [9]. The theory is valid for steady state and transient operations as well as for generic waveforms of voltage and current. The transformation of the currents i_1, i_2, i_3 to i_0, i_α, i_β is given by (7) and the real power p, imaginary power q and the zero sequence power p_o are given by (8):

$$\begin{bmatrix} i_\alpha \\ i_\beta \\ i_0 \end{bmatrix} = \sqrt{\frac{2}{3}} \begin{bmatrix} 1 & -1/2 & -1/2 \\ 0 & \sqrt{3}/2 & -\sqrt{3}/2 \\ 1/\sqrt{2} & 1/\sqrt{2} & 1/\sqrt{2} \end{bmatrix} \cdot \begin{bmatrix} i_1 \\ i_2 \\ i_3 \end{bmatrix} \quad (7)$$

$$\begin{bmatrix} p \\ q \\ p_0 \end{bmatrix} = \begin{bmatrix} 0 & v_\alpha & v_\beta \\ 0 & v_\beta & -v_\alpha \\ v_0 & 0 & 0 \end{bmatrix} \cdot \begin{bmatrix} i_0 \\ i_\alpha \\ i_\beta \end{bmatrix} \quad (8)$$

Where:

i_α, i_β - α-axis and β-axis current components.
i_0 - Zero-sequence current component.
v_α, v_β - α-axis and β-axis voltage components.
v_0 - Zero-sequence voltage component.

If the three-phase grid voltage is balanced, it is composed of positive-sequence components at fundamental frequency. The three-phase grid voltages and the load currents are measured and transformed to α-β-0 coordinates. Using (8), p, and q are calculated, but in this case p_o is null because the voltage is balanced. Supposing that in the load there are positive-sequence components at fundamental frequency and harmonics, the real power and imaginary power will have constant and oscillating components [9].

Since the grid currents must have a sinusoidal waveform and be in phase with the grid voltage in the proposed design, the reference imaginary power for the inverter is the total imaginary power calculated in (8). The reference real power responsible to compensate harmonics (p_{Lr}) is composed of the oscillating load component (Fig. 2).

The reference real power is also composed of reference power to control the dc link voltage (p_{dcr}) and reference photovoltaic array power (p_r). Calculating the reference powers it is possible to determine the reference currents:

$$\begin{bmatrix} i_{\alpha r} \\ i_{\beta r} \end{bmatrix} = \frac{1}{v_\alpha^2 + v_\beta^2} \begin{bmatrix} v_\alpha & v_\beta \\ v_\beta & -v_\alpha \end{bmatrix} \cdot \begin{bmatrix} p_{Lr} + p_{dcr} - p_r \\ q_L \end{bmatrix} \quad (9)$$

Where:

$i_{\alpha r}$, $i_{\beta r}$ - α-axis and β-axis reference currents.
p_{Lr}, p_{dcr}, p_r- Reference real power.

The control is based on the model in the $\alpha\beta$ frame and (10) and (11) in Fig. 2 are

$$d_\alpha = \frac{v_\alpha - u_\alpha}{V} \quad (10)$$

$$d_\beta = \frac{v_\beta - u_\beta}{V} \quad (11)$$

Where:

$v_{n\alpha}$, $v_{n\beta}$ - α -axis, β -axis normalized reference voltages.
u_α, u_β - Outputs of the current PI compensators.

Subtracting the load real power of the filtered load real power, the value is used as the reference real power since the positive current flows into the inverter. The inverter dc link voltage controller calculates the power to maintain the dc link voltage by passing the dc link voltage error through a PI compensator. The power of the MPPT controller corresponds to the real power available from the photovoltaic array.

IV. MAXIMUM POWER POINT TRACKING

It is important to operate the photovoltaic system near the maximum power point to increase the efficiency of photovoltaic arrays. A MPPT method often used is the perturbation and observation method [10]. However, in this paper, it is used the slope of power versus voltage, which decreases the oscillation problem and it is easy to implement [1]. The output power of the PV array and the differential of the output power to the output voltage can be expressed as

$$P = V \cdot I \quad (12)$$

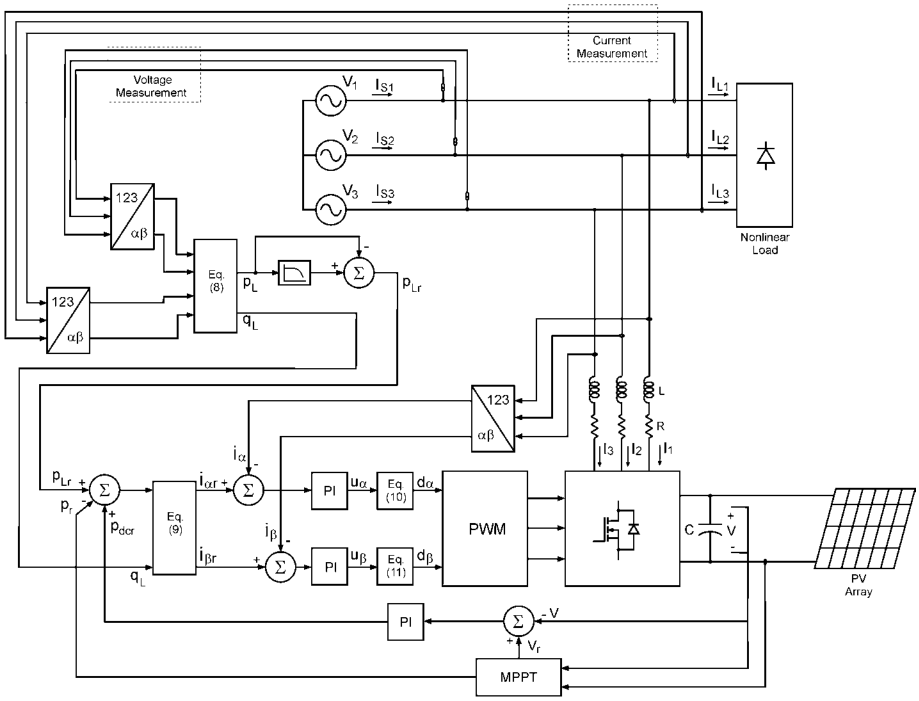

Fig. 2. Block diagram of the instantaneous reactive power based controller for the proposed system.

$$\frac{dP}{dV} = I + \frac{\Delta I}{\Delta V} \cdot V \quad (13)$$

Where:

- P - PV array output power.
- V - PV array output voltage.
- I - PV array output current.
- ΔI - Increment of the PV array output current.
- ΔV - Increment of the PV array output current.

In the method, (13) is used as the index of the maximum power point tracking operation (Fig. 3). When *dP/dV<0*, decreasing the reference voltage forces *dP/dV* to approach zero; when *dP/dV>0*, increasing the reference voltage forces *dP/dV* to approach zero; when *dP/dV=0*, reference voltage does not need any change [1]. Fast changes in the solar irradiation (*S*) are simulated and the PV array voltage follows the reference voltage generated by the MPPT algorithm (Fig. 4). The small oscillation around the reference voltage shows the good performance of the system.

V. PWM TECHNIQUES

Space vector modulation (SVM) is nowadays the most used PWM technique to control inverters.

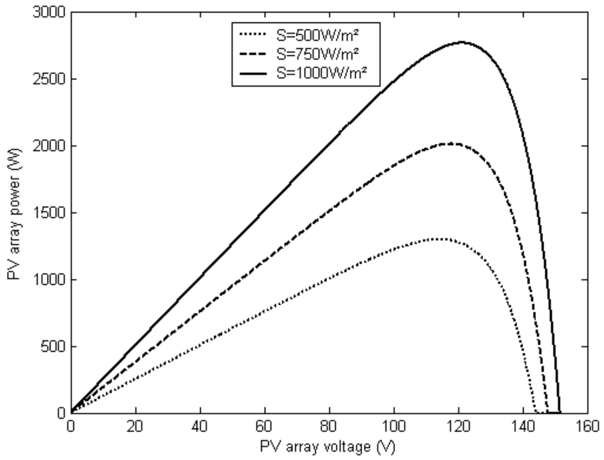

Fig. 3. Characteristic diagram of the solar array

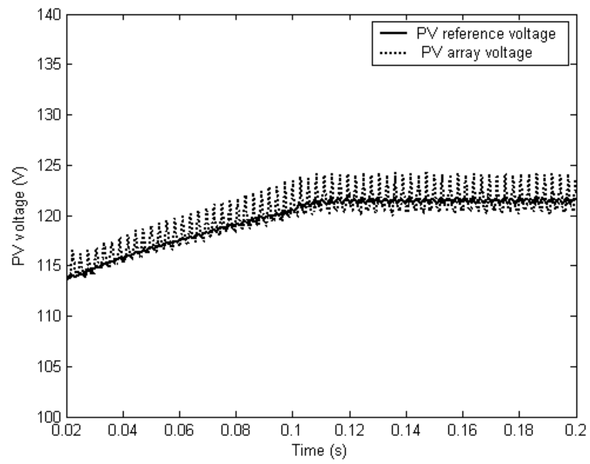

Fig. 4. MPPT controller: PV array output voltage

In the space vector PWM (SVPWM), each phase is switched in sequence by switching only one inverter leg at each transition from one state to the next one. One possibility to reduce the number of switching is to use the two-phase modulation in which only two phases are modulated while the third phase is clamped to the positive (DPWMMIN) or negative (DPWMMAX) dc rail [11].

SVM techniques can also be implemented by using digital scalar PWM. In this approach, non-sinusoidal modulating waveforms are introduced in a simple way. In digital scalar PWM the split and distribution of the zero space vectors duration $V_0(t_{01})$ and $V_7(t_{02})$, inside the sampling interval, can be represented by the apportioning factor $\mu = t_{01} / (t_{01} + t_{02})$ [12]. When $0 < \mu < 1$ the modulation is known as continuous modulation. The case μ=0.5 is equivalent to SVPWM. When μ = 0 (DPWMMAX) or μ = 1 (DPWMMIN) the modulation is known as discontinuous modulation. Because of the simple implementation, the scalar PWM is used to control the inverters.

VI. SIMULATION RESULTS

If the three-phase grid voltage is balanced and undistorted, the SRF based controller and the IRP based controller can compensate current harmonic and reactive power effectively as shown in Fig. 5 and in Fig. 6.

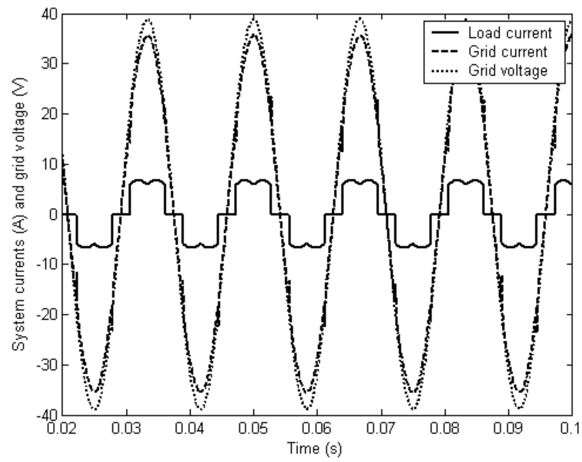

Fig. 5. Current harmonic and reactive power compensations (SRF)

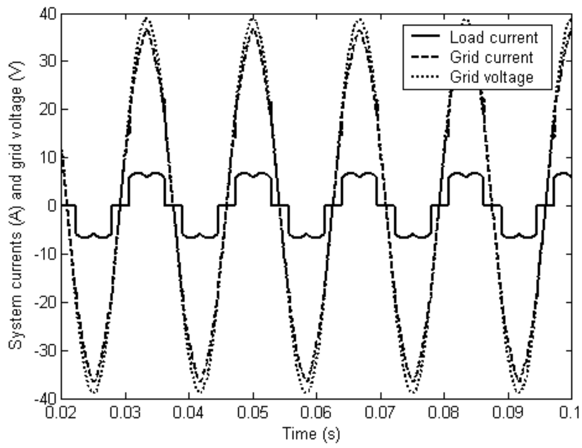

Fig. 6. Current harmonic and reactive power compensations (IRP)

Figures 5 and 6 show the negative of the grid current because it is generated more power from the PV array than that needed for the load. Therefore, in this case the PV array supplies the load and injects power for the grid. The simulation conditions that have been used for the system and the controllers are shown in Table I.

The MPPT algorithm presents very good results with 99.81% of the PV maximum output power for the SRF based controller and 99.86% for the IRP based controller. The THD of the grid currents is 2.34% for the SRF based controller and is 2.35% for the IRP based controller. The differences between the controllers are small when changing the method.

Based on results, the criteria to be used to compare the controllers for the PV conversion system is the operation under distorted grid voltage. The SRF based controller is almost insensitive to grid voltage distortions, since any non-dc component in the SRF can be attributed to harmonics in steady state [13]. The IRP based controller has problems with the grid voltage distortion, since the product of grid voltage and load current will result in real power contained at the harmonic frequencies. This real power contained at harmonic frequencies will result in a distorted grid current [13].

The simulated results shown that the SRF method (Fig. 7) presents better performance than the IRP method (Fig. 8) when the grid voltage is distorted. The MPPT algorithm presents very good results for both controllers (around 99.8%). The THD of the grid currents is 6.69% for the SRF based controller and is 7.62% for the IRP based controller. Therefore the SRF method is chosen to control the inverter.

TABLE I
Simulation conditions for the SRF and IRP controllers

Conditions	SRF based controller	IRP based controller
Solar irradiation (*S*)	1000W/m^2	1000W/m^2
Grid rms voltage	220V	220V
Transformer	220V/27.5V	220V/27.5V
Inductance (*L*)	1mH	1mH
Capacitance (*C*)	300μF	300μF
Load power	415W	415W
Current loop integral gain	30500	31000
Current loop proportional gain	10	45
Voltage loop integral gain	125	500
Voltage loop proportional gain	0.4	40
PWM technique	DPWMMAX	DPWMMAX

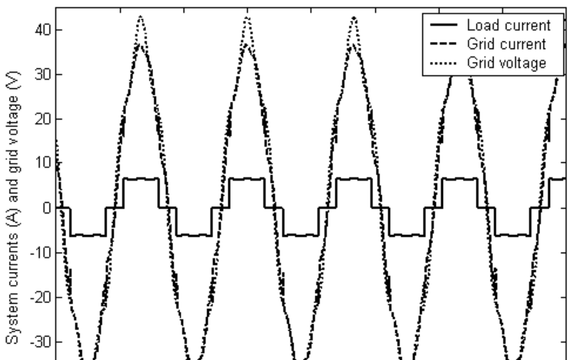

Fig. 7. Compensations with distorted grid voltage (SRF).

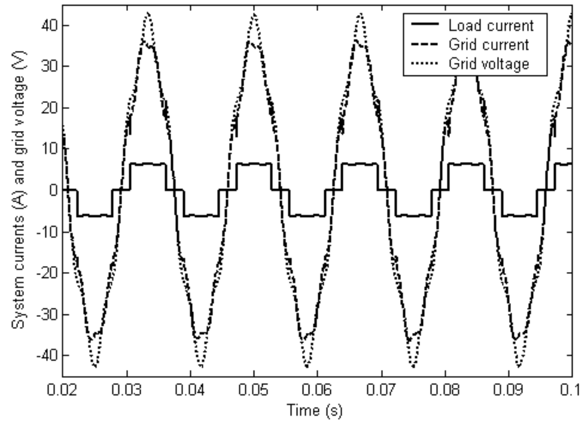

Fig. 8. Compensations with distorted grid voltage (IRP).

To verify the design of the proposed conversion system, simulations using different loads were realized. Inverter efficiencies have been calculated in Table II from the component models used with curve fitting techniques [14] for the conditions listed in the table. DPWMMIN and DPWMMAX present the best efficiencies among the PWM techniques. It is expected since that only two phases are modulated at each modulation interval for those techniques. The MPPT algorithm presents very good results with at least 99.68% of the PV maximum output power. The THD of the grid currents is kept below 3.7% for all situations. The sinusoidal PWM (SPWM) presents the highest THD.

Based on discussed characteristics, the criteria to be used to compare PWM techniques for the PV conversion system is the inverter efficiency since the differences among the MPPT efficiencies are very small when changing the PWM technique. Also, except the SPWM, the differences among the THD of the system currents are very small when changing PWM. Therefore for the proposed design, DPWMMIN or DPWMMAX should be used to improve efficiency. In Fig. 9, the load fundamental current and the grid fundamental current are used as magnitude 1 and they are not shown to allow that the harmonics can be better analyzed. The simulation conditions are shown in Table I.

VII. CONCLUSION

The proposed system provides photovoltaic generation, current harmonic compensation and reactive power compensation simultaneously. The maximum power point tracking controller allows reaching the maximum power point very rapidly.

TABLE II
Efficiency for different PWM techniques (SRF controller)

PWM	MPPT efficiency	Inverter efficiency	Grid current THD	Load
SPWM	99.79%	94.02%	2.73%	THD 29.88% Power 415W
SVPWM	99.81%	94.03%	2.48%	
DPWMMIN	99.73%	95.26%	2.36%	
DPWMMAX	99.81%	95.32%	2.34%	
SPWM	99.77%	95.23%	3.63%	THD 29.88% Power 542W
SVPWM	99.68%	95.08%	3.19%	
DPWMMIN	99.68%	96.12%	3.23%	
DPWMMAX	99.80%	96.16%	3.30%	

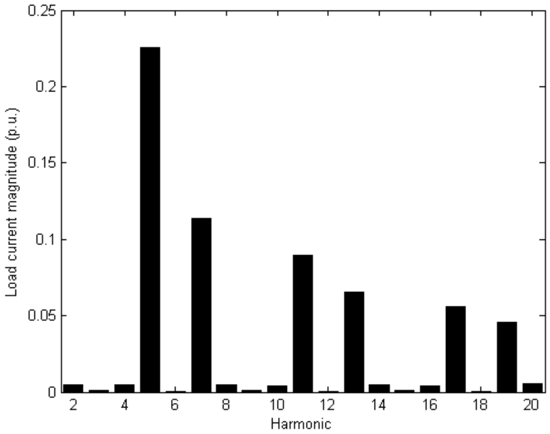

(a) Harmonics in the load current

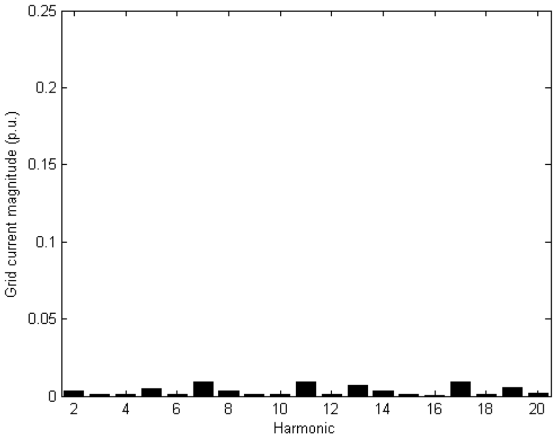

(b) Harmonics in the grid current (SRF based controller)

Fig. 9. Harmonics in the load current and in the grid current

Using simulation results, it is possible to make a comparative study of different possibilities of control. A synchronous reference frame based controller is compared to an instantaneous reactive power based controller. The controllers have been tested under balanced grid voltage conditions. In presence of undistorted grid voltage the controllers work very well, but in presence of distorted grid voltage, the synchronous reference frame method presents better performance than the instantaneous reactive power method. Therefore the synchronous reference frame method is chosen to control the three-phase inverter.

The proposed design has been used to make a comparative study of PWM techniques. The photovoltaic generation system for a three-phase grid using only one inverter associated with the best PWM technique increases efficiency.

ACKNOWLEDGEMENT

The authors thank Conselho Nacional de Desenvolvimento Científico e Tecnológico (CNPq) for its financial support.

REFERENCES

[1] Y. C. Kuo, T. J. Liang, and J. F. Chen, "Novel maximum power-point-tracking controller for photovoltaic energy conversion system", *IEEE Trans. on Industrial Electronics*, vol. 48, no. 3, pp. 594-601, May/June 2001.

[2] L. G. Leslie, Jr., Design and analysis of a grid connected photovoltaic generation system with active filtering function, Master Thesis, Virginia Polytechnic Institute and State University, Blacksburg, Virginia – USA, 2003.

[3] A.B. Maish, C. Atcitty, S. Hester, "Photovoltaic system reliability", *IEEE Photovoltaic Specialists Conference*, pp.1049-1054, 1997.

[4] W.I. Bower, H. Thomas, "Balance-of-system improvements for photovoltaic applications resulting from the PVMaT 4A1 program", *IEEE Photovoltaic Specialists Conference*, pp. 1093-1096, 1997.

[5] B. Lindgren, "Topology for decentralized solar energy inverters with a low voltage ac-bus," European Conference on Power Electronics and Applications, 1999.

[6] B.K. Bose, P.M. Szczesny and R.L. Steigerwald, "Microcomputer control of a residential photovoltaic power conditioning system", *IEEE Trans. on Industry Applications*, vol. 21, no.5, pp. 1182-1191, September/October 1985.

[7] S.J. Chiang, K.T. Chang and C.Y. Yen, "Residential photovoltaic energy storage system", *IEEE Trans. on Industrial Electronics*, vol. 45, no.3, pp. 385-394, May/June 1998.

[8] N. Mendalek and K. Al-Haddad, "Modeling and nonlinear control of shunt active power filter in the synchronous reference frame," *IEEE Harmonics and Quality of Power International Conference*, pp. 30-35, 2000.

[9] H. Akagi, Y. Kanazawa and A. Nabae, "Instantaneous reactive power compensator comprising switching devices without energy storage components", *IEEE Trans. on Industry Applications*, vol. 20, no.3, pp. 625-630, May/June 1984.

[10] C. Hua, J. Lin, and C. Shen, "Implementation of a DSP-controlled photovoltaic system with peak power tracking," *IEEE Trans. on Industrial Electronics*, vol. 45, no. 1, pp. 99-107, January/February 1998.

[11] A. M. Hava, R. J. Kerkman, and T. A. Lipo, "Simple analytical and graphical tools for carrier based pwm methods," *IEEE Power Electronics Specialists Conference*, pp.1462-1471, 1997.

[12] C. B. Jacobina, A. M. N. Lima, E. R. C. da Silva, R. N. C. Alves, and P. F. Seixas, "Digital scalar pulse width modulation: a simple approach to introduce non-sinusoidal modulating waveforms," *European Conference on Power Electronics and Applications*, pp. 100-105, 1997.

[13] S. Bhattacharya and D. Divan, "Synchronous frame based controller implementation for a hybrid series active filter system", *IEEE Industry Applications Conference*, pp. 2531-2540, 1995.

[14] M. C. Cavalcanti, E. R. C. da Silva, D. Boroyevich, W. Dong, and C. B. Jacobina, "Comparative evaluation of losses in soft and hard-switched inverters," *IEEE Industry Applications Conference*, pp. 1912-1917, 2003.